EasyChair Preprint

№ 9306

Observation Theory and Result Analysis of Sea Surface Wind Speed by Pulse Radar

Yiyang Luo, Vladislav Lutsenko, Sergey Shulga, Irina Lutsenko and Anh Nguyen

November 28, 2022

Observation theory and result analysis of sea surface wind speed by pulse radar

Yiyang Luo
Department of theoretical radiophysics
V. N. Karazin Kharkiv National University
Kharkiv, Ukraine
yiyangluo@163.com

Vladislav Lutsenko
Department of Radiophysicintroscopy
O. Ya. Usikov Institute for Radiophysics and Electronics of NASU
Kharkiv, Ukraine
vladislavlutsenko1953@gmail.com

Sergey Shulga
Department of theoretical radiophysics
V. N. Karazin Kharkiv National University
Kharkiv, Ukraine
sergeyshulga@karazin.ua

Irina Lutsenko
Department of Radiophysicintroscopy
O. Ya. Usikov Institute for Radiophysics and Electronics of NASU
Kharkiv, Ukraine
irene-lutsenko@ukr.net

Xuan-Anh Nguyen
Department of atmosphere physics
Institute of Geophysics of Vietnam
Academy of Science and Technology
Hanoi, Vietnam
nxuananh05@gmail.com

***Abstract*— The mechanism of detection of sea surface height and wind speed using pulsed radar is elucidated. Associated methods and test equipment were developed. A comparative experiment is carried out, and some conclusions with practical application value are drawn by controlling the equipment parameters of the pulse radar. Partial differential and polar transformations were applied to extract the RCS features of the sea surface in the centimeter and millimeter wave bands.**

Keywords*— *coordinate system transformation, partial differential, pulse radar, RCS, remote sensing, spectrogram

I. Introduction

Most modern weather radars are pulse-Doppler radars, which can monitor the distribution and intensity of precipitation. This data can be used to analyze the structure of the storm and whether it can cause severe weather in the future. During World War II, military radar operators noticed echo noise from weather factors such as rain, snow, freezing rain, etc. After the war, the original military scientists were able to continue to study how to use those echoes, and David Atlas of the United States developed the first practical weather radar [1].

The US National Severe Storm Laboratory was established in 1964 to study the application of dual polarization signals and the Doppler effect to weather radars. In May 1973, a tornado hit Union City, Oklahoma. The lab's 10cm-band Doppler weather radar recorded the entire life cycle of a tornado for the first time. This finding uncovered a mesoscale vortex in the high-altitude clouds before tornadoes: the Tornado vortex signature, which led the US National Weather Service to recognize that Doppler weather radars are excellent tornado forecasting devices. And the devastating devastation caused by the super-outbreak of the tornado on April 3 and 4, 1974, made Doppler radar research even more funded. From 1980 to 2000, meteorological radar networks were widely established in developed countries such as North America, Europe, and Japan. Doppler radars, which can detect the moving speed of particles in the atmosphere, also replaced traditional radars that can only detect the position and intensity of weather systems. In 1988, the United States officially carried out the construction of the 10cm band weather radar network, which was called the next-generation weather radar or Weather Service Radar 1988 Doppler (WSR-88D) [2].

After 2000, dual-polarization techniques became practical, increasing the availability of information about effective precipitation types (eg, the contrast between rain and snow). "Dual polarization" refers to microwave radiation capable of transmitting and receiving both horizontally polarized waves and vertically polarized waves. The weather radar is connected to the waveguide through a cavity magnetron or klystron, and then connected to a parabolic antenna to directionally emit microwave pulses into space. The wavelength of microwaves emitted by weather radars is in the range of 1-10 cm, which is roughly 10 times the diameter of raindrops or ice crystals. At this frequency, the Rayleigh scattering effect is the strongest. This ensures that part of the energy of the radar wave can be reflected from the particle surface back to the direction of the radar station [3].

The microwave dual-polarization pulsed radar was tested and applied in our research. Radar waves propagate outward from the radar station in the form of spherical waves. This causes the volume of space traversed by the radar wave to increase with the distance from the radar station at the same time, so the angular resolution of the radar decreases. For our application scenario (scanning and observing wind and waves on the sea surface), the detection range of our pulse radar is set to 5 kilometers.Corresponding analytical methods by means of partial differential equations and coordinate system transformations were developed.

II. Devices and Theory

In our research, **Ka-band, Ku-band and X-band Pulse radars** were used, of which main technical characteristics of the measuring systems are given in Table.I, and the appearance of antenna systems is shown in Fig.1.

a) **b)**

Fig. 1. Pulse radars with a cyclic view of space: a) - radar antennas with wavelengths of 2 cm (Ku-band in the background) and 3 cm (X-band); b) radar with a wavelength of 8 mm (Ka-band).

TABLE I. TECHNICAL CHARACTERISTICS OF PULSE RADAR WITH SCANNING

Technical characteristics	*Parameters*		
Wavelength, cm	*3*	*2*	*0,8*
Pulse power, kW	*70*	*1*	*10*
Pulse duration, ns	*50*	*400*	*66*
Width of RP *in azimuth, mrad* *in elevation, mrad*	 *10* *55*	 *30* *55*	 *10* *34*
Threshold sensitivity, W	*10-11*	*10-12*	*3*10-12*
Antenna dimensions in azimuth, cm	*350*	*60*	*80*
Space survey speed, deg/s	*180; 600*	*4;8*	*360*
Scanning sector, hail	*360*	*240*	*36*
Repetition frequency, kHz	*4*	*4*	*7,5*
Polarization	*V, H*	*V*	*V*

Pulse radars with a cyclic view of space. To study the spatial characteristics in range and azimuth of the radar image of the sea surface, dummies of pulsed centimeter and millimeter wave radars with circular and sector scanning modes in azimuth and digital signal recording equipment were used. When developing the measuring systems, commercially available radar stations of the centimeter and millimeter wave ranges were taken as a basis. At a wave of 3 cm, the transmitter of the "Don" ship navigation radar with a modernized microwave part was used. A parabolic mirror 3.5 m in diameter with a dually polarized feed and the ability to change the scanning speed from 30 rpm to 100 rpm was used as an antenna. To reduce aerodynamic drag, the antenna system was enclosed in a cylindrical fairing rotating with itself - Fig. 1a. At a wavelength of 2 cm, the "Credo" coherent pulse radar was used, which is used as a short-range reconnaissance station in normal mode, and at a wavelength of 8 mm, the incoherent "Val" radar was used in normal mode to illuminate the ground situation.

At the first stage of the experiments, the registration of the radar image of the sea surface was carried out by photographing the radar indicator, then a digital radar image recorder was developed. The output signals of the pulse radar were fed to a digital data recorder, which ensured its recording at a clock frequency of 13 MHz (the size of the resolution element in range was about 11.3 m) and viewing the recorded information in the form of a frame of brightness marks, as well as in the oscilloscope mode.

The recorder was controlled and information was processed by a microcomputer. In the interactive mode, the recorder made it possible to set the initial delay, the number of readings recorded in range, the number of recorded pulses in a burst, the number of bursts and the number of gaps between them. The flexible capabilities of the recorder made it possible to use it to record radar signals with significantly different technical characteristics.

The description of the radar field of interference from the sea on orthogonal polarizations can be based on a two-scale model of scattering from the sea surface [4, 5]:

$$\dot{N}_2(t,r)=\dot{G}(t,r)\dot{s}_2(t,r);\dot{N}_1(t,r)=\dot{G}(t,r)\dot{s}_1(t,r) \qquad (1)$$

where indices 1, 2 - show which reception polarization refers to: index 1 - consistent with the emitted, 2 - orthogonal; $\dot{N}_i(t,r)$ denote the complex amplitudes of the sea-scattered signal at $i \in (1, 2)$ polarizations, due to scattering by resonant ripples $\dot{s}_i(t,r)$, which are located on a large gravity wave $\dot{G}(t,r)$, leading to both amplitude and phase modulation of the scattered signal.

The **wave height** depends on its driving force, and the driving force depends on the pressure per unit area. Then, depending on the wind speed, different wind pressures will produce different driving forces. A simple understanding is that wind speed determines wind pressure, and wind pressure determines wave height. According to the wind-pressure relationship derived from Bernoulli's equation, the dynamic pressure of wind is:

$$wp=0.5\cdot\rho_0\cdot v^2, \qquad (2)$$

where wp is wind pressure [kN/m^2], ρ_o is air density [kg/m^3], v is wind speed [m/s]. $\rho_o=\rho/g$. Under standard conditions (air pressure 1013 hPa, temperature 15 ° C) , the air gravity is ρ=0.01225 [kN/m^3]. The gravitational acceleration g=9.8 [m/s^2] at 45 ° latitude, then we get $wp=v^2/1600$ and this formula can be used as a general estimation. Similarly, the microwave coherent interference feature about the height of the sea wave also corresponds to the wind pressure wp on the plane perpendicular to the airflow direction, and then the corresponding wind speed feature can be converted.

The waves of the sea are the periodic up and down movement of the ocean on a certain scale, resulting in obvious wave crests and troughs. This gives the surface of the ocean a never-quiet, ever-changing picture. Such waves are formed due to the interaction between the flowing air and the surface of the ocean. Once the ripples are present, the wind pushes on their sides, making them higher. The ripples evolve into waves that push the water far beyond the equilibrium surface. When this happens, under the force of gravity, the water sinks. Inertia causes the sinking water to drop below the equilibrium level.

Since the target within the detection range is not unique, the basic **radar equation** must be modified as follows [6,7]:

$$P_r=\left[P_t\frac{G^2\lambda^2\sigma_0}{(4\pi)^3R^4}\right]\propto\frac{\sigma_0}{R^4}, \qquad (3)$$

where, P_r represents the receiving power; P_t represents the transmitting power; G represents the antenna gain; λ represents the wavelength of the radar wave; σ_0 is the effective radar cross-sectional (RCS) area of the target; R refers to the distance between the radar station and the target.

Considering that the ocean waves are composed of water droplets, the effective radar cross-sectional areas of all target cells (water particles) must be added together [7]. Consider further our research object: the sea surface is a surface distribution target.

$$\sigma_0=S\bar{\sigma}_0,\ S=\left[\frac{c\tau}{2}\right]\cdot[R\theta], \qquad (4)$$

where, S represents the scanned square, which is the product of pulse length and beam width; $\bar{\sigma}_0$ represents the average RCS area per unit of sea surface; c represents the speed of light; τ represents the pulse period; θ is the pulse width in radians.

Fig. 2. Schematic diagram of the working of pulse radar in different scenarios (near shore/offshore).

Combining formulas (3) and (4) , the following formulas are obtained:

$$P_r = \left[P_t \frac{G^2 \lambda^2}{(4\pi)^3 R^4}\right] \cdot \left[\frac{c\tau}{2}\right] \cdot [R\theta] \cdot \overline{\sigma_0} = \left[P_t \tau G^2 \lambda^2 \theta\right] \cdot \left[\frac{c}{128\pi^3}\right] \cdot \frac{\overline{\sigma_0}}{R^3} \quad (5)$$

It can be obtained from the above formula:

$$P_r \propto \frac{\overline{\sigma_0}}{R^3}, \quad (6)$$

which represents that the echo strength of the radar is inversely proportional to R^3 rather than R^4. In order to be able to compare echo data at different distances, this ratio must to be used to convert, which is very important for subsequent correct and reasonable studies on radar map about reflection of ocean waves.

III. Algorithms and Results

In order to ensure the reliability of the experiment and the diversity of application scenarios of the studied method, the radar was placed on the beach/ near the shore and on the boat for measurement, and the polarization mode and scanning speed were adjusted/controlled respectively. The schematic diagram is shown in Fig.2, and the obtained more detailed results can be compared and analyzed. It should be noted that the experimental results show that the reciprocating scanning of the same sector is useless and harmful, which will blur the radar image.

Further, the processing algorithm/flow of the obtained radar data/image is shown in Fig.3. It should be mentioned that the application of the simple spatio-temporal spectrum analysis method is not feasible here. According to the previous experimental attempts, the spectrum method for azimuth and distance is difficult to obtain an effective measure of spatial frequency. For the actual situation analysis of ocean waves, distance conversion (6) and Cartesian coordinate conversion are necessary. After the necessary two steps, the radar image can be regarded as a real-world image that reflects the distribution of real ocean wave intensity (wave height). Further by taking partial derivatives, the relevant wind speed, wind direction and wind energy are calculated/estimated.

The results of the radar images obtained at different stages of the algorithm are shown in Fig.4, Fig.5 and Fig.6.

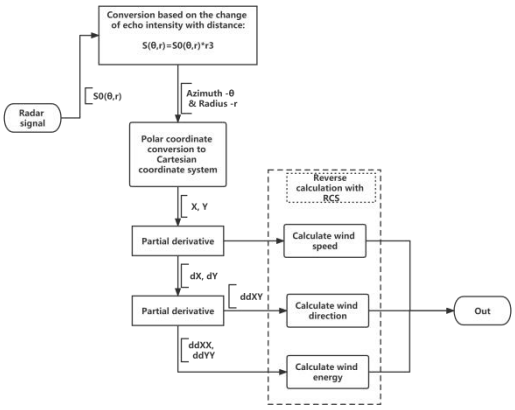

Fig. 3. Algorithm structure diagram of the working of pulse radar in our research

A. Comparison of Results for Radar-Scan near the Coast and in the Sea

Under the same wind speed of 7m/c (2-3 Beaufort scale), the energy distribution of waves measured in the sea is multi-source (multi-directional) and relatively strong. The energy distribution of the waves measured on the shore is unidirectional (pointing towards the Coast), which is in line with reality. The result was shown in Fig.4.

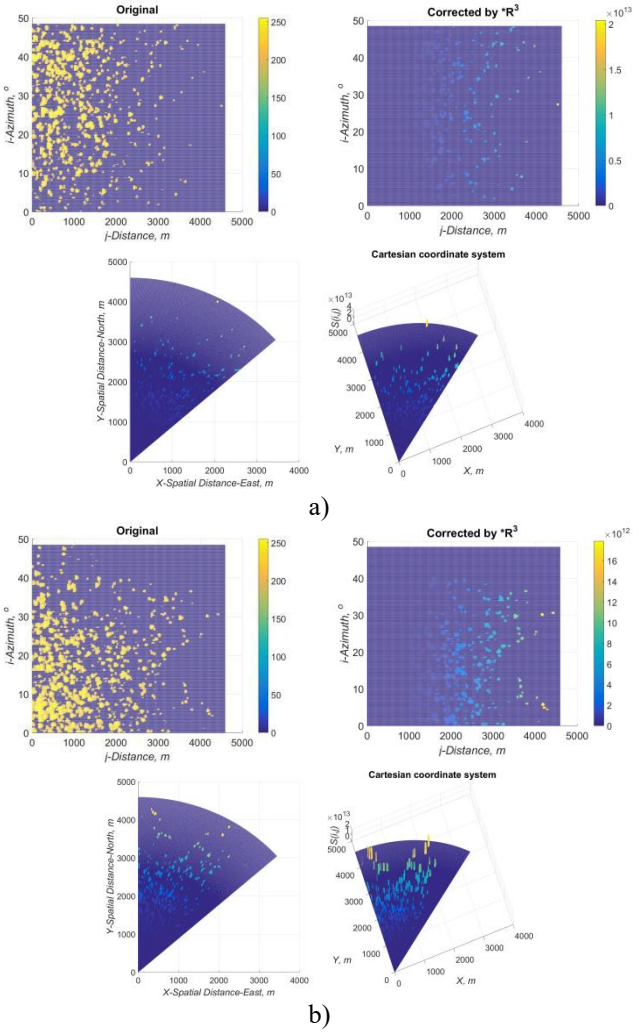

Fig. 4. Results for Radar-Scan (the sector range 0-48.6°) using vertical polarization near the Coast (a) and in the Sea (b).

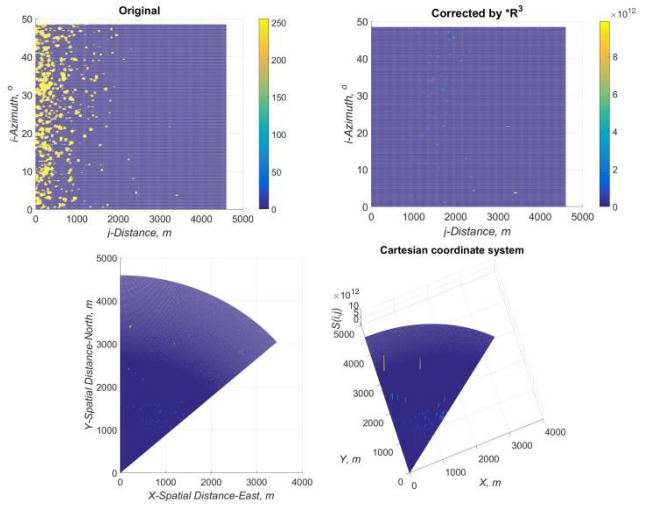

Fig. 5. Results for Radar-Scan (the sector range 0-48.6º) using horizontal polarization near the Coast.

B. *Comparison of Results for Vertical and Horizontal Polarization*

Under the same conditions (close to the shore and wind speed 1), the radar image Fig.5 obtained with horizontal polarization is significantly different from the radar image Fig.4a obtained with vertical polarization. The radar image produced with the help of the horizontal polarization has less number and energy of the echo signal.

The pulsed signal produced by horizontal polarization can be likened to a cork on water. That is, the entire mass of water that makes up its wave moves with the ocean wave, but throw a cork into the water and you'll see it bob up and down as the wave goes by, it doesn't move with the wave. This is because in an ideal wave, a water particle would move in a circular motion. The diameter of the circle is largest at the surface of the ocean, where it is equal to the amplitude of the waves. As the depth increases, the diameter of the circle gradually decreases until the wave does not move until the depth is about half the wavelength (called the wave base). When a storm blows over an area, it produces many different wave trains, each with a different wavelength. Because wave trains travel away from the source at different speeds, they separate from each other as they move away from the source, a phenomenon known as wave dispersion.

C. *Compare Results at Different Scan Ranges (with or without Annihilation Taken into Account)*

When the scanning range is expanded shown as Fig.6, the acute angle sector Fig.4b that the radar scans does not change significantly. When the scanning angle is close to 90 degrees, there is obvious signal annihilation (no echo), which is unique to vertical polarization (horizontal polarization does not).

Shown in Fig.6b is the radar image obtained through the X and Y partial derivatives (second-order partial derivatives), which essentially reflect the wave height corresponding to the wind energy that caused the waves. Ocean waves appear as isolated waves on radar images, and these waves are sharpened and extracted by partial derivatives. These isolated waves constitute the fronts of the drift of the entire ocean wave caused by external driving forces (wind, tides, and currents).

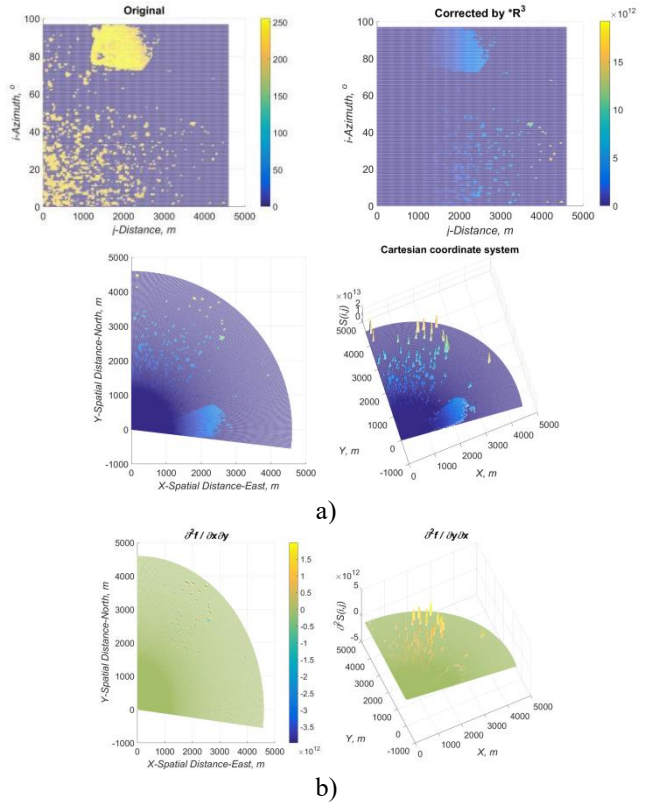

Fig. 6. Results for Radar-Scan (the sector range 0-97.2º) using vertical polarization in the Sea

With this method, some isolated waves with similar dynamic characteristics in the wave group are concentrated, and these similar wave crests can be fused (local integration) to obtain the front of the wave, and then the wind direction can be estimated.

IV. Conclusion

After the correction of the echo signal, the information contained in the long-distance target reflected signal was fully excavated and displayed, and can be used as a medium- and long-distance sea state prediction. With the help of partial differentiation, wind speed, wind direction and wind energy related to wave movement can be revealed and estimated from radar images. Also by means of second-order partial differentials in the spatial X &Y directions, the signal annihilation due to vertical polarization can be eliminated.

References

[1] David Atlas, "Radar in Meteorology", published by American Meteorological Society.

[2] Susan Cobb. Weather radar development highlight of the National Severe Storms Laboratory first 40 years. NOAA Magazine. NOAA. October 29, 2004.

[3] R. J. Doviak, ; D. S. Zrnic. Doppler Radar and Weather Observations Second. San Diego California: Academic Press. 1993.

[4] A. I. Kalmykov, A. I. Kalmykov, I. E. Ostrovsky, A. D. Rozenberg, and I. M. Fuks. Influence of the sea surface structure on the spatial characteristics of the radiation scattered by it, Izv. universities. Radiophysics. - 1965.- T. VIII, No. 6. - S. 1117-1127

[5] A. A. Zagorodnikov. Radar survey of sea waves from aircraft / A. A. Zagorodnikov. - L .: Gidrometeoizdat, 1978. - 239 p.

[6] R. J. Doviak, D. S. Zrnic. Doppler Radar and Weather Observations Second. San Diego California: Academic Press, 1993.

[7] Merrill I. Skolnik. Radar Handbook, Third Edition. McGraw-Hill Education, 2008